DFT Analysis of Porous Lewis Acids Catalysts for Biomass Conversion to Fuels and Chemicals

Brian D. Montejo-Valencia, PhD[1]
[1]Universidad Ana G Mendez at Gurabo, e-mail: montejob1@uagm.edu

Abstract– Density functional theory (DFT) calculations can guide the design of efficient and selective catalysts for converting biomass-derived feedstocks to fuels and chemicals. In this work, we performed systematic DFT calculations with specific treatment of van der Waals forces to analyze the structure and functionality of zeolites substituted with metals. The catalytic activity of Sn-BEA and the interaction of this catalyst with different solvents were studied. Through these calculations, we intended to analyze the effect of solvent on the reaction mechanism to turn fructose into dihydroxyacetone (DHA) and glyceraldehyde (GLA). The interactions of reactants, products, and solvent molecules with Sn-BEA will provide insight into the catalytic properties of these systems, and transition state calculations will guide on the selection of the best solvent for this reaction.

Keywords—DFT, Zeolite, Biomass

I. Introduction

Lignocellulosic biomass is a raw material composed of cellulose, hemicellulose, and lignin.[1] From this raw material, high-value chemicals such as lactic acid can be obtained.[2] The conversion of biomass into sugars begins with acid hydrolysis for the separation of its three main components. Two sugars that can be obtained are glucose and fructose. Glucose is in chemical equilibrium with fructose and can be converted to lactic acid or methyl lactate using functionalized zeolites such as Sn-BEA as shown in Figure 1.[3]–[7]
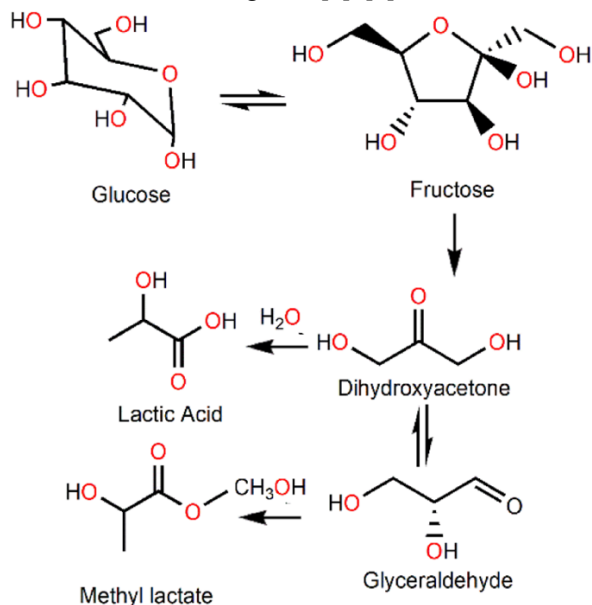

Figure 1 Mechanism for the conversion of glucose to lactic acid and methyl lactate using Sn-BEA

Lactic acid is used as a precursor to produce syndiotactic polylactide which is used as a biodegradable plastic. In the food industry, it is used to ferment milk and produces sour foods like kumis and yogurt. On the other hand, it is also used as a component in different cleaning products as a descaling agent to remove hard water deposits. In the cosmetics industry, it is used to produce water-soluble lactates.[8]

Zeolites are microporous minerals composed mainly of silicon and oxygen. There is a great variety of types of zeolites, so far more than 200 types have been discovered, with only 40 found naturally and the rest produced synthetically in the laboratory. They have many uses such as agriculture, aquaculture, and livestock. In agriculture, it is used to improve soil water retention, in aquaculture to control ammonia levels in the water, and in livestock to improve feed conversion in animals. They are also used as catalysts by adding different metals such as tin and titanium to accelerate different types of reactions such as the one studied in this article for the conversion of glucose to lactic acid.[9]

Since glucose is directly obtained from biomass hydrolysis, much effort has been put forth into understanding how glucose interacts and reacts on Sn-BEA. Previous studies have focused on the analysis of the mechanism for the isomerization of glucose to fructose [10]–[15]. Despite the significant progress made to elucidate the mechanism for the conversion of glucose to fructose, further studies are still necessary to clarify the mechanisms for the rest of the reaction (e.g. fructose conversion to glyceraldehyde and Dihydroxyacetone). As far as we know only our work published in 2019 has proposed a possible mechanism for this reaction.[10] Although the energy barriers reported in this mechanism are high (266 kJ/mol), here we analyzed the interaction of different solvents with Sn-BEA and study how energy barriers are affected by various solvents.

II. Methodology

In this work the mechanisms for converting fructose to GLA and DHA in Sn-BEA using various solvents were analyzed using periodic DFT calculations. β-D-fructofuranose (FF) was used as the conformer of fructose. We analyzed the polymorphism A of zeolite beta and use the coordinates as reported by the International Zeolite Association (IZA).[11] BEA has a tetragonal unit cell with lattice parameters: a = b = 12.6 Å and c = 26.2 Å, and has nine crystallographic sites. Metal substituted BEA zeolites (M BEA) were analyzed with Sn. The calculations were performed using the Vienna ab initio simulation package (VASP 5.4)[12], [13] with the generalized

gradient approximation Perdew–BurkeErnzrhof (PBE)[14], [15] exchange-correlation. Standard PAW[16] potentials were used for all the elements, except for the Sn atom, for which higher electronic PAW pseudopotentials were used instead of the default ones. Thus, for the substituted Sn, we employed Sn_d to treat it semicore s as a valence state. The dispersion interactions were considered with the DFT-D3 method.[17] The Brillouin zone sampling was restricted to the G-point. The energy cutoff was set to 500 eV. Full geometry optimizations were performed with fixed cell parameters. The nudged elastic band method (NEB)[18]–[20] was used to determine the minimum energy path and to locate the transition-state (TS) structures. Then, the climbing image NEB and the dimer methods were used to obtain the saddle point. The TS was confirmed by frequency calculations involving only the motions of the atoms of the adsorbed molecules, as well as the Sn substituted with its four bonded oxygens. Figure 2 shows the unit cell of the Sn-BEA zeolite.
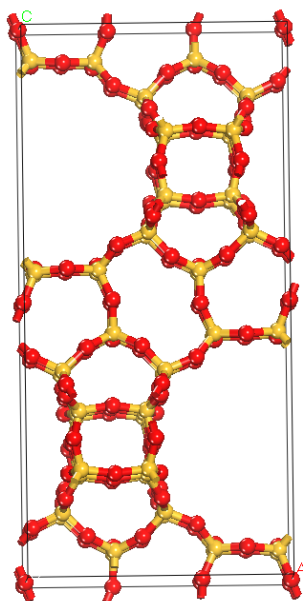

Figure 2 Unit cell of the Sn-BEA zeolite

To analyze the effect of the solvent on energy barriers, single-point calculations were performed with Gaussian using VASP's optimized geometries. Single points implicitly consider the effect of the solvent using a polarizable continuum model based on the dielectric constant of the solvent. Cluster models were obtained in Gaussian by cutting the periodic structure. The boundary Si atoms were saturated with hydrogen atoms, which were aligned on the same direction of the removed oxygen atoms. The Si−H bonds were maintained at 1.5000 Å. All the results were obtained using the functional ωB97XD, which is a long-range corrected functional. A mix of basis sets were used in the calculations involving the preferential substitution site.

The Pople basis set 6- 31+g** was used for Si, O, C, and H atoms, whereas the effective core potentials MWB4625 was used for Sn. Figure 3 shows the cluster model used in Gaussian for the Sn-BEA.
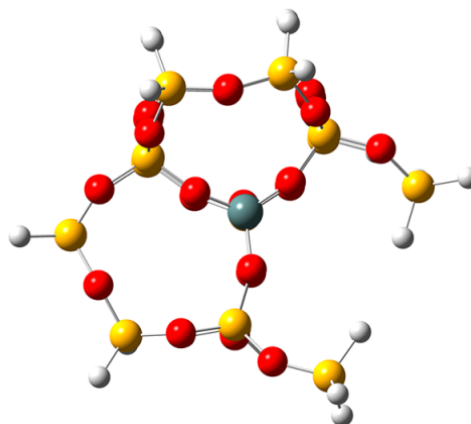

Figure 3 Cluster model used in Gaussian for the Sn-BEA.

III. RESULTS AND DISCUSSION

The work performed through these computational resources guides the design of efficient catalysts for obtaining fuels and chemicals from biomass-derived molecules. Periodic density functional theory (DFT) calculations with long-range corrections are being used to analyze the opening of the fructose catalyzed by Sn-BEA. We have previously proposed a mechanism for the conversion of fructose to dihydroxyacetone (DHA) and glyceraldehyde (GLA). Here we propose to quantify the effect of the solvent on the reaction energies and energy barriers.

We have calculated the mechanism for the opening of the fructose ring with several metals-substituted zeolites in vacuum. Figure 4 a,b illustrates two plausible reaction mechanisms for the opening of the fructose ring. In the mechanism of Figure 4a, the intramolecular hydrogen shift occurs in one elementary step (B → C). In the reaction mechanism of Figure 4b the intramolecular hydrogen shift occurs through the zeolite and involves two elementary steps (B' → I1 → C'). The reactions energies for the fructose ring opening by the two mechanisms proposed in Figure 4 are shown in Figure 5 a,b.
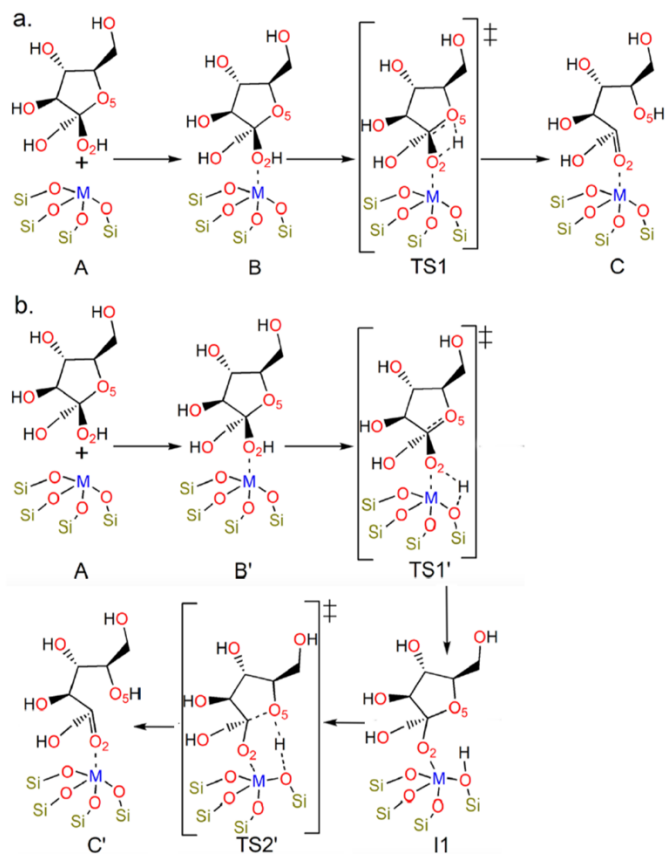
Figure 4 Reaction mechanisms for fructose ring opening through (a) one and (b) two elementary steps
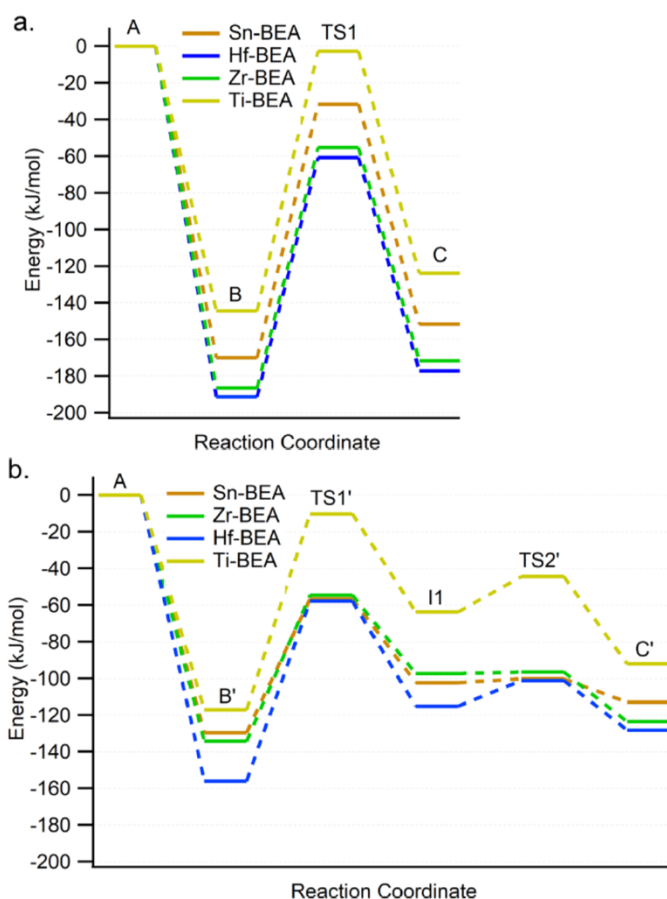

Figure 5 Reaction energies of the opening of the fructose ring on M-BEA through (a) the one-step mechanism shown in Figure 4 and (b) through the two-step mechanism shown in Figure 4b

Based on Figure 5a, the lowest apparent activation energy for the opening of fructose is on Hf-BEA, followed by Zr-BEA, Sn-BEA, and Ti-BEA. In the second proposed mechanism, shown in Figure 4b, the hydrogen is shifted from O2 to O5 through two consecutive steps. The energy barriers obtained for the first step (B' → I1) increase as follows: Sn-BEA (73.1 kJ/mol) > Zr-BEA (79.7 kJ/mol) > Hf-BEA (98.2 kJ/mol) > Ti-BEA (107.0 kJ/mol). The second elementary step in the mechanism of Figure 4b (I1 → C′) involves the formation of adsorbed acyclic fructose. This step consists of the shift of the hydrogen atom from the zeolite to O5, which is an oxygen atom in the adsorbed molecule. The reaction has a low energy barrier for all of the zeolites ranging from 0.84 kJ/mol for Zr-BEA to 19.2 kJ/mol for Ti-BEA.

When comparing the energies obtained in Figure 5, we note that for all of the M-BEA catalysts analyzed here, the energy barriers obtained for the one-step mechanism shown in Figure 4a are higher than the ones obtained for the two-step mechanism shown in Figure 4b. These results suggest that the opening of the cyclic fructose ring to form the acyclic fructose is more favorable through the two-step mechanism.

Furthermore, among all the metal-substituted zeolites analyzed in this work, Sn-BEA yields the lowest energy barrier for the opening of the fructose ring.

The mechanism for producing glyceraldehyde (GLA) and dihydroxyacetone (DHA) is shown in Figure **6**. The open ring of fructose changes from being adsorbed through oxygen O2 to being adsorbed through oxygen O4. Subsequently, hydrogen passes from carbon C2 to carbon C4. The energies of the vacuum mechanism can be seen in figure 7 for Sn-BEA.
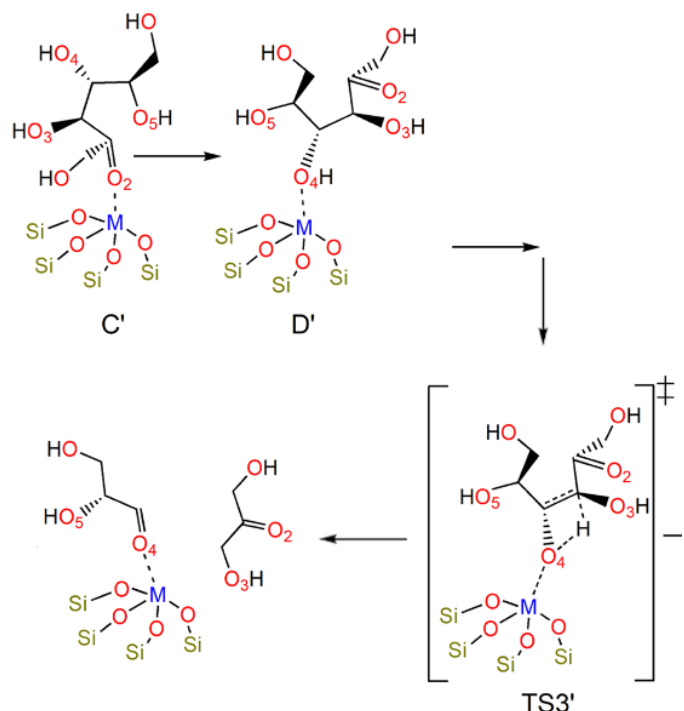

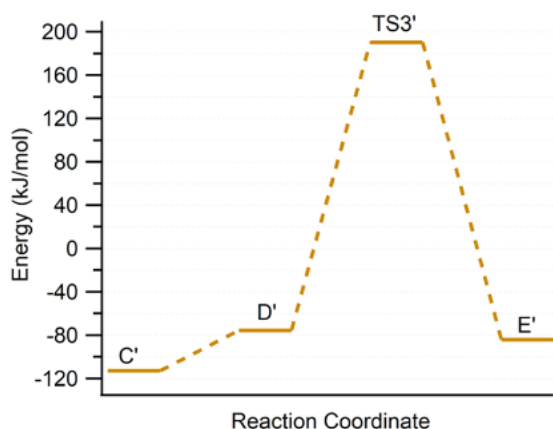Figure 6. Reaction mechanism for the conversion of open fructose to DHA and GLA

Figure 7. Reaction energies for the conversion of acyclic fructose toDHA and GLA.

As can be seen in Figure 7, the energy barrier of the reaction is quite high, so the reaction would not occur through this mechanism. Therefore, energy barriers and reaction energies were calculated for different solvents. The results are shown in Table 1 and were obtained by implicitly considering the solvent using a Polarizable Continuum Model. These results demonstrate that the energy barrier decreases as the dielectric constant of the solvent is lower.

Table 1 Energy barriers and reaction energies for the hydride shift between C2 and C4 in the isomerization of glucose to fructose

Solvent	ε	E_{TS} (kJ/mol)	E_{rxn} (kJ/mol)
Vacuum (VASP)		92.75	-3.05
Vacuum (Gaussian)		90.41	-7.65
Heptane	1.9	93.04	-5.16
Benzene	2.3	93.70	-4.49
Toluene	2.4	93.86	-4.32
Diethyl ether	4.2	95.81	-2.22
Chloroform	4.7	96.12	-1.87
Chlorobenzene	5.7	96.63	-1.28
Aniline	6.9	97.10	-0.72
THF	7.4	97.28	-0.51
Dichloromethane	8.9	97.67	-0.03
Acetone	20.5	98.98	1.66
Ethanol	24.8	99.19	1.96
Methanol	32.6	99.44	2.32
Acetronitrile	35.7	99.51	2.42
Water	78.4	99,97	3.10

Figure 8 shows the relationship between the dielectric constant of several solvents with their respective energy barriers for the hydride shift step. Our calculations suggest that there is a logarithmic relationship between the energy barriers and the dielectric constant of the solvent.

Figure 9 shows the reaction energies for the hydride shift step for several solvents with respect to reagents in vacuum. The energy of solvation increases as the dielectric constant of the solvents increases, with water being the solvent with greater solvation while heptane is the least. By analyzing the effect of solvation with energy barriers for each solvent, we can conclude that, the greater the solvation, the greater the energy barrier.
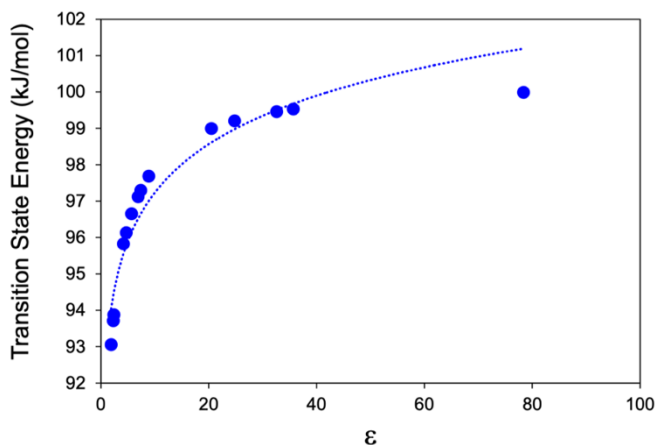
Figure 8 Relationship between the dielectric constant of several solvents with their respective energy barriers for the hydride shift step
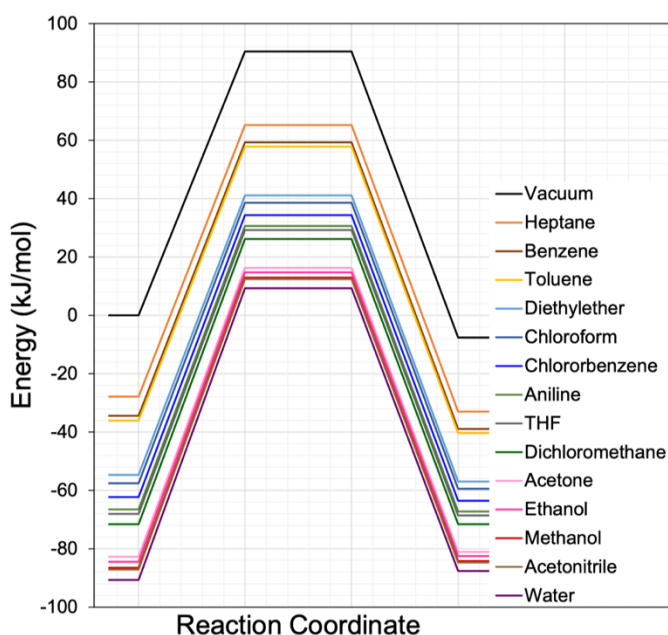

Figure 9 Reaction energies for the hydride shift step for several solvents with respect to the reagents in vacuum

V. CONCLUSION

Based on our result, the lowest apparent activation energy for the opening of fructose in one step is on Hf-BEA, followed by Zr-BEA, Sn-BEA, and Ti-BEA. The energy barriers for the two-step mechanisms are lower than the energies obtained for the one-step mechanisms. For the two steps mechanism, Sn-BEA shows the lowest energy barrier between the metal zeolites studied.

Our results also demonstrate that the energy barrier decreases as the dielectric constant of the solvent is lower and the energy of solvation increases as the dielectric constant of the solvents increases.

V. FUTURE WORK

The polarizable continuum model used in this work does not consider the direct interaction of the solvent molecules with the transition state. Thus, in future work, the solvent molecules will be explicitly in the calculations to study the solvent's interaction with this reaction.

REFERENCES

[1] C.-H. Zhou, X. Xia, C.-X. Lin, D.-S. Tong, and J. Beltramini, 'Catalytic conversion of lignocellulosic biomass to fine chemicals and fuels.', *Chem Soc Rev*, vol. 40, no. 11, pp. 5588–617, 2011, doi: 10.1039/c1cs15124j.

[2] D. Klemm, B. Heublein, H. P. Fink, and A. Bohn, 'Cellulose: Fascinating biopolymer and sustainable raw material', *Angewandte Chemie - International Edition*, vol. 44, no. 22, pp. 3358–3393, 2005, doi: 10.1002/anie.200460587.

[3] C. M. Lew, N. Rajabbeigi, and M. Tsapatsis, 'Tin-containing zeolite for the isomerization of cellulosic sugars', *Microporous and Mesoporous Materials*, vol. 153, pp. 55–58, 2012, doi: 10.1016/j.micromeso.2011.12.020.

[4] W. Dong *et al.*, 'Selective Chemical Conversion of Sugars in Aqueous Solutions without Alkali to Lactic Acid Over a Zn-Sn-Beta Lewis Acid-Base Catalyst', *Sci Rep*, vol. 6, no. January, p. 26713, 2016, doi: 10.1038/srep26713.

[5] M. S. Holm, S. Saravanamurugan, and E. Taarning, 'Conversion of sugars to lactic acid derivatives using heterogeneous zeotype catalysts.', *Science*, vol. 328, no. 5978, pp. 602–605, 2010, doi: 10.1126/science.1183990.

[6] C. M. Osmundsen, M. S. Holm, S. Dahl, and E. Taarning, 'Tin-containing silicates: structure-activity relations', *Proceedings of the Royal Society A: Mathematical, Physical and Engineering Sciences*, vol. 468, pp. 2000–2016, 2012, doi: 10.1098/rspa.2012.0047.

[7] M. Moliner, Y. Román-Leshkov, and M. E. Davis, 'Tin-containing zeolites are highly active catalysts for the isomerization of glucose in water', *Proceedings of the National Academy of Sciences*, vol. 107, no. 14, pp. 6164–6168, 2010, doi: 10.1073/pnas.1002358107.

[8] F. A. Castillo Martinez, E. M. Balciunas, J. M. Salgado, J. M. Domínguez González, A. Converti, and R. P. de S. Oliveira, 'Lactic acid properties, applications and production: A review', *Trends in Food Science and Technology*, vol. 30, no. 1. pp. 70–83, Mar. 2013. doi: 10.1016/j.tifs.2012.11.007.

[9] M. E. Davis, 'Zeolites from a materials chemistry perspective', *Chemistry of Materials*, vol. 26, no. 1. pp. 239–245, Jan. 14, 2014. doi: 10.1021/cm401914u.

[10] M. J. Cordon, J. N. Hall, J. W. Harris, J. S. Bates, S. J. Hwang, and R. Gounder, 'Deactivation of Sn-Beta zeolites caused by structural transformation of hydrophobic to hydrophilic micropores during aqueous-phase glucose isomerization', *Catal Sci Technol*, vol. 9, no. 7, pp. 1654–1668, 2019, doi: 10.1039/c8cy02589d.

[11] P. Dugkhuntod *et al.*, 'Synthesis and Characterization of Sn, Ge, and Zr Isomorphous Substituted MFI Nanosheets for Glucose Isomerization to Fructose', *Chempluschem*, vol. 87, no. 1, Jan. 2022, doi: 10.1002/cplu.202100289.

[12] Y. Román-Leshkov, M. Moliner, J. A. Labinger, and M. E. Davis, 'Mechanism of glucose isomerization using a solid lewis acid catalyst in water', *Angewandte Chemie - International Edition*, vol. 49, no. 47, pp. 8954–8957, 2010, doi: 10.1002/anie.201004689.

[13] Y. P. Li, M. Head-Gordon, and A. T. Bell, 'Analysis of the reaction mechanism and catalytic activity of metal-substituted beta zeolite for the isomerization of glucose to fructose', *ACS Catal*, vol. 4, no. 5, pp. 1537–1545, 2014, doi: 10.1021/cs401054f.

[14] G. Yang, E. a Pidko, and E. J. M. Hensen, 'The mechanism of glucose isomerization to fructose over Sn-BEA zeolite: a periodic density functional theory study.', *ChemSusChem*, vol. 6, no. 9, pp. 1688–96, Sep. 2013, doi: 10.1002/cssc.201300342.

[15] R. Bermejo-Deval *et al.*, 'Metalloenzyme-like catalyzed isomerizations of sugars by Lewis acid zeolites', *Proceedings of the National Academy of Sciences*, vol. 109, no. 25, pp. 9727–9732, 2012, doi: 10.1073/pnas.1206708109.

[16] B. D. Montejo-Valencia and M. C. Curet-Arana, 'Periodic DFT Study of the Opening of Fructose and Glucose Rings and the Further Conversion of Fructose to Trioses Catalyzed by M-BEA (M = Sn, Ti, Zr, or Hf)', *Journal of Physical Chemistry C*, vol. 123, no. 6, 2019, doi: 10.1021/acs.jpcc.8b10211.

[17] 'International Zeolite Association (IZA).' http://europe.iza-structure.org/IZA-SC/ftc_fw.php?STC=MFI (accessed Aug. 19, 2016).

[18] G. Kresse, 'From ultrasoft pseudopotentials to the projector augmented-wave method', *Phys Rev B*, vol. 59, no. 3, pp. 1758–1775, 1999, doi: 10.1103/PhysRevB.59.1758.

[19] G. Kresse and J. Hafner, 'Ab initio molecular-dynamics simulation of the liquid-metal–amorphous-semiconductor transition in germanium', *Phys Rev B*, vol. 49, no. 20, pp. 14251–14269, 1994, doi: 10.1103/PhysRevB.49.14251.

[20] J. P. Perdew, K. Burke, and M. Ernzerhof, 'Generalized Gradient Approximation Made Simple', *Phys. Rev. Lett.*, vol. 78, no. 1992, p. 1396, 1997, doi: 10.1103/PhysRevLett.78.1396.

[21] J. P. Perdew and Y. Wang, 'Accurate and simple analytic representation of the electron-gas correlation energy', *Phys. Rev. B*, vol. 45, pp. 13244–13249, 1992.

[22] P. E. Blochl, 'Projector Augmented-Wave Method', *Phys Rev B*, vol. 50, no. 24, pp. 17953–17979, 1993, doi: 10.1103/PhysRevB.50.17953.

[23] S. Grimme, J. Antony, S. Ehrlich, and H. Krieg, 'A consistent and accurate ab initio parametrization of density functional dispersion correction (DFT-D) for the 94 elements H-Pu', *Journal of Chemical Physics*, vol. 132, p. 154104, 2010, doi: 10.1063/1.3382344.

[24] G. Henkelman and H. Jónsson, 'A dimer method for finding saddle points on high dimensional potential surfaces using only first derivatives', *Journal of Chemical Physics*, vol. 111, no. 15, pp. 7010–7022, 1999, doi: 10.1063/1.480097.

[25] A. Ulitsky and R. Elber, 'A new technique to calculate steepest descent paths in flexible polyatomic systems', *J. Chem. Phys.*, vol. 92, no. 1990, pp. 1510–1511, 1990, doi: 10.1063/1.458112.

[26] G. Mills, H. Jónsson, and G. Schenter, 'Reversible work transition state theory: application to dissociative adsorption of hydrogen', *Surf Sci*, vol. 324, no. 2–3, pp. 305–337, 1995, doi: 10.1016/0039-6028(94)00731-4.